The Journal of Antibiotics (2016) 69, 524–533

www.nature.com/ja

ORIGINAL ARTICLE

Biosynthetic potential of sesquiterpene synthases: product profiles of Egyptian Henbane premnaspirodiene synthase and related mutants

Hyun Jo Koo[1,3], Christopher R Vickery[1,2,3], Yi Xu[1], Gordon V Louie[1], Paul E O'Maille[1], Marianne Bowman[1], Charisse M Nartey[1], Michael D Burkart[2] and Joseph P Noel[1]

The plant terpene synthase (TPS) family is responsible for the biosynthesis of a variety of terpenoid natural products possessing diverse biological functions. TPSs catalyze the ionization and, most commonly, rearrangement and cyclization of prenyl diphosphate substrates, forming linear and cyclic hydrocarbons. Moreover, a single TPS often produces several minor products in addition to a dominant product. We characterized the catalytic profiles of *Hyoscyamus muticus* premnaspirodiene synthase (HPS) and compared it with the profile of a closely related TPS, *Nicotiana tabacum* 5-*epi*-aristolochene synthase (TEAS). The profiles of two previously studied HPS and TEAS mutants, each containing nine interconverting mutations, dubbed HPS-M9 and TEAS-M9, were also characterized. All four TPSs were compared under varying temperature and pH conditions. In addition, we solved the X-ray crystal structures of TEAS and a TEAS quadruple mutant complexed with substrate and products to gain insight into the enzymatic features modulating product formation. These informative structures, along with product profiles, provide new insight into plant TPS catalytic promiscuity.
The Journal of Antibiotics (2016) **69,** 524–533; doi:10.1038/ja.2016.68; published online 22 June 2016

INTRODUCTION

Terpenoids are one of the largest groups of naturally produced chemicals, widespread across all three domains of life.[1,2] Plants in particular encode an incredible diversity of terpenoid biosynthetic pathways that produce molecules conferring flavor, fragrance, antimicrobial, attractive and repellent properties to plants.[3,4] Terpenoids from plants also possess a wide variety of antibiotic,[5] antiparasitic[6] and antifungal[7] activities, as well as chemotherapeutic properties for the treatment of various human maladies.[8] Class I terpene synthases (TPSs) are classified as mono-, sesqui- and di-terpene synthases according to their catalytically preferred substrates geranyl diphosphate, farnesyl diphosphate (FPP) and geranylgeranyl diphosphate, respectively.[1] Products are formed via rearrangement of a cationic intermediate arising from cleavage of the C-O bond between the diphosphate moiety and the carbon chain.[9] This allylic carbocation intermediate can undergo a variety of structural alterations before arriving at a final product (Figure 1).[10] Generally, TPSs produce several minor products in addition to one or more abundant products.[11]

Previously, a detailed product profile for the TPS 5-*epi*-aristolochene synthase (TEAS) from common tobacco (*Nicotiana tabacum*) was described.[12] The observed minor products likely reflected key cationic intermediates en route to the major product 5-*epi*-aristolochene (**1**).[13] Egyptian henbane (*Hyoscyamus muticus*) premnaspirodiene synthase (HPS) (also known as vetispirodiene synthase),[14] a TPS sharing 75.5% identity with TEAS, produces premnaspirodiene (**2**) (also known as vetispiradiene) as a major product. In addition to some overlap in product profiles, the source plants of HPS and TEAS share a common evolutionary lineage in the Solanaceae family of plants.[15] Therefore, HPS and TEAS serve as reliable extant models for catalytic diversification from a shared ancestor. However, the minor product profile of HPS has not been previously characterized. In order to mechanistically interrogate the diverging enzymatic properties linking HPS and TEAS structurally and functionally, we characterized the full product profile of HPS.

The product profiles of TEAS and HPS are sensitive to the identities of nine amino acid residues on and surrounding the active site surface.[15,16] Mutating these nine positions in TEAS to the corresponding HPS residues yields TEAS-M9 that produces premnaspirodiene (**2**) as its major product. Conversely, HPS-M9 produces 5-*epi*-aristolochene (**1**) as its major product.[16] We also investigated the product profiles of these two interconverted mutants. Comparison of HPS, TEAS, HPS-M9 and TEAS-M9 product profiles reveals intriguing information regarding active

[1]Howard Hughes Medical Institute, The Salk Institute for Biological Studies, Jack H Skirball Center for Chemical Biology and Proteomics, La Jolla, CA, USA and [2]Department of Chemistry and Biochemistry, University of California, San Diego, La Jolla, CA, USA
[3]Co-first authors.
Correspondence: Dr HJ Koo or Professor JP Noel, Howard Hughes Medical Institute, The Salk Institute for Biological Studies, Jack H Skirball Center for Chemical Biology and Proteomics, 10010 North Torrey Pines Road, La Jolla, CA 92037, USA.
E-mail: hjk@salk.edu or noel@salk.edu
Received 19 April 2016; revised 3 May 2016; accepted 7 May 2016; published online 22 June 2016

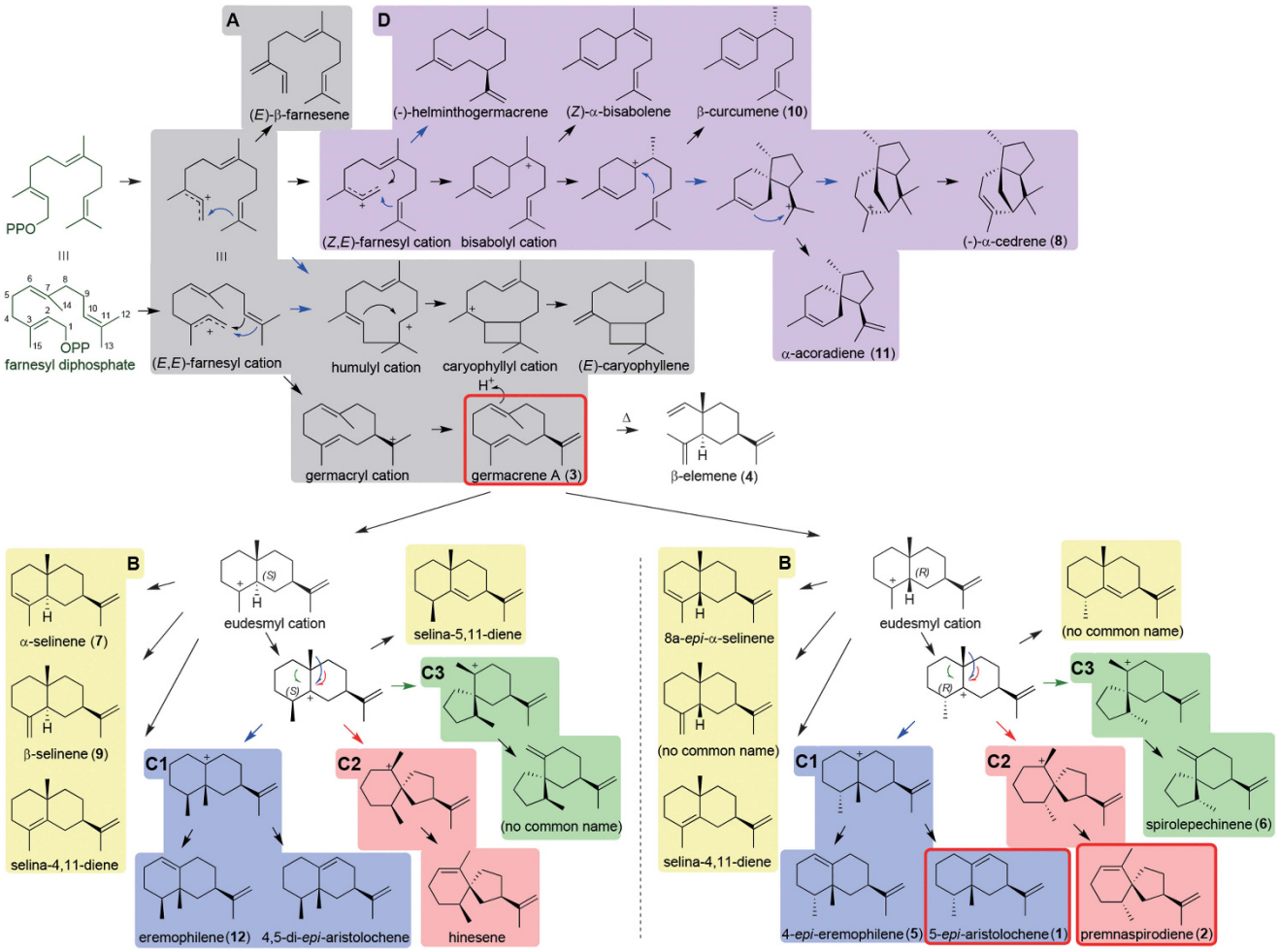

Figure 1 Chemical pathways leading to products formed by *Nicotiana tabacum* 5-*epi*-aristolochene synthase (TEAS) and *Hyoscyamus muticus* premnaspirodiene synthase (HPS) from farnesyl diphosphate (FPP). Class A (gray) arises from early quenching of the carbocation; class B (yellow) derives from the eudesmyl cation without an alkyl migration; classes C1, C2 and C3 are from the eudesmyl cation with three different alkyl migrations; and class D products are from the (*Z,E*)-farnesyl cation. Products at the bottom of the figure are separated into those arising from the two possible stereoisomers of the cationic intermediate stemming from germacrene A. Highlighted in red boxes are key intermediate germacrene A and the two major products of TEAS and HPS, 5-*epi*-aristolochene and premnaspirodiene, respectively. Compounds are numbered according to their appearance in the main text.

site properties that confer product profile diversity in otherwise orthologous enzymes.

Biosynthesis of minor products by TPSs increases at high temperature[12,17] or extreme pH,[17,18,19] accompanied by an overall decrease in total terpenoid products formed. In addition, widely varying temperatures may also modulate TPS activity *in planta*.[20] In some cases, previously formed minor products are produced at higher levels than the major products with changes in enzyme reaction conditions.[17] However, it is not clear whether formation of minor products is more, less or equally dependent on active site dynamics of the TPS or the altered chemical reactivity of substrates and intermediates at elevated temperatures and pH. Temperature and pH screens of all four HPS and TEAS constructs were carried out to assess these environmental perturbations on terpenoid product formation. Finally, in order to provide structural underpinnings for the initial steps of product formation in the TEAS–HPS family, we determined X-ray crystal structures of TEAS containing several small molecule ligands. These TPS structures, along with product profiling of these four closely related TPSs using a variety of conditions, provide architectural details linking active site organization with product formation and chemical diversity.

MATERIALS AND METHODS

Protein expression and purification

TEAS, TEAS-M9, HPS and HPS-M9 were cloned into the pHIS9GW vector and expressed in BL21 (DE3) at 18 °C for 16 h with 0.5 mM isopropyl β-D-1-thiogalactopyranoside (IPTG) induction, as previously reported.[12] Harvested cells were resuspended in lysis buffer (50 mM Tris-HCl, pH 8.0, 500 mM NaCl, 20 mM imidazole, 10% (v/v) glycerol, 1% (v/v) Tween-20 and 20 mM β-mercaptoethanol), lysed by sonication and centrifuged to recover soluble proteins. Soluble proteins were mixed with Ni-NTA resin (Qiagen, Hilden, Germany) for 1 h, then washed twice with 10 bed volumes of wash buffer (50 mM Tris-HCl, pH 8.0, 500 mM NaCl, 20 mM imidazole, 10% (v/v) glycerol and 20 mM β-mercaptoethanol) and eluted with 3 bed volumes of elution buffer (50 mM Tris-HCl, pH 8.0, 500 mM NaCl, 250 mM imidazole, 10% (v/v) glycerol and 20 mM β-mercaptoethanol). Purified proteins were dialyzed in dialysis buffer I (50 mM Tris-HCl, pH 8.0, 500 mM NaCl and 10 mM β-mercaptoethanol) with thrombin at 4 °C for 18 h and passed over Ni-NTA and Benzamidine Sepharose (GE Healthcare, Little Chalfont, UK) columns to remove uncleaved His-tagged protein and thrombin, respectively. His-tag removed proteins were further

purified to homogeneity by size exclusion chromatography. Purified fractions were combined and dialyzed in dialysis buffer II (12.5 mM Tris-HCl, pH 8.0, 50 mM NaCl and 2 mM DTT) followed by concentration using Amicon Ultra 30 000 molecular weight cutoff centrifugal filters (Millipore, Billerica, MA, USA) before storage at 9.8–25.5 mg ml^{-1} at −80 °C.

Enzyme assays

(*E*,*E*)-Farnesyl diphosphate (FPP) was purchased from Isoprenoids.com (Tampa, FL, USA). In general, for comparing product profiles, enzyme assays were carried out in 500 µl, including 100 µl of Protein Extraction Buffer (50 mM 3-Morpholino-2-hydroxypropanesulfonic acid (MOPSO), pH 7.0, 10% (v/v) glycerol, 5 mM $MgCl_2$, 5 mM DTT, 5 mM sodium ascorbate and 0.5 mM phenylmethylsulfonyl fluoride), and using 0.1–0.5 µM enzyme and 25–50 µM FPP overlaid with 500 µl hexane. After incubating overnight at 30 °C, the reactions were vortexed, allowed to separate and the hexane layers were recovered and concentrated by gaseous nitrogen flow. *p*-Chlorotoluene (SUPELCO, Bellefonte, PA, USA) was included in all organic phases as an internal standard. For analysis, a Hewlett-Packard 6890 GC coupled to a 5973 mass selective detector was used with either an HP-5MS or an HP-Chiral column (Agilent, Santa Clara, CA, USA). Products were identified by comparison with previous product characterization spectra, Massfinder 4.0 software (Hamburg, Germany), and by comparison with authentic standards.

For measurements of steady-state kinetics, 500 µl reactions containing 10 mM BIS-TRIS propane (BTP), pH 7.0, 5 mM $MgCl_2$, varying FPP concentrations and 5 nM TPSs were used overlaid with 500 µl hexane containing *p*-chlorotoluene (SUPELCO), the internal standard. Four time points (3.3, 8, 16 and 32 min) for 8 different FPP concentrations (0.78, 1.56, 3.125, 6.25, 12.5, 25, 50 and 100 µM) were assayed. After incubations at room temperature, the reaction mixtures were vortexed, phase separated and the top layer of hexanes injected onto a Hewlett-Packard 6890 GC coupled to a 5973 mass selective detector with an HP-5MS column (Agilent) in splitless mode. Sums of product peak areas from each GC chromatogram were calculated using mass selective detector ChemStation E.02.02.1431 (Agilent), and these values converted into product concentrations by reference to internal standards. Initial velocities were plotted as a function of FPP concentration. From these graphs, Michaelis–Menten kinetics including V_{MAX} and K_M values were derived using GraphPad Prism (GraphPad Software, San Diego CA, USA, www.graphpad.com) and apparent k_{cat} values were calculated (V_{MAX}/[enzyme]/min).

Enzyme assays at varying temperatures

Assay solutions (497.5 µl) included 100 µl of Protein Extraction Buffer (see above) and 0.5 µM enzyme and were overlaid with 500 µl hexane. Each reaction was prepared on ice and incubated for 4 min at pre-set temperatures in a water bath, then 2.5 µl of 10 mM FPP (final 50 µM in 500 µl volume) was added to the aqueous phase. Reactions were incubated for 1.5 h and products were recovered as described above.

Heat inactivation and Thermofluor analyses

For heat inactivation, 1.25 µM of the TPSs were used in 20 µl reaction volumes that included 4 µl of Protein Extraction Buffer (see above). Glycerol can protect enzymes from the effects of heating. All TPS samples are stored in 50% (v/v) glycerol at varying protein concentrations. Therefore, various concentrations of glycerol were first tested for their effects on heat treatments. Up to 1% (v/v) glycerol in TPS solutions did not alter heat inactivation experiments (Supplementary Figure 1). Therefore, glycerol concentrations during heat inactivation were fixed to 1% (v/v) in all samples. Heat inactivation was carried out in a preheated thermocycler, and sample tubes were immediately moved to ice after the designated times. Enzyme assays of heat-treated TPSs were carried out in a total volume of 500 µl, including 20 µl of heat-treated enzymes (final 0.05 µM), 100 µl of Protein Extraction Buffer (see above) and 25 µM FPP. Reactions were overlaid with 500 µl hexane and incubated for 45 min. Thermofluor assays were performed using a Lightcycler 480 (Roche, Basel, Switzerland) with 3 µM of TPSs, 10 mM BTP buffer (pH 5.4–10.6), 6.25 mM $MgCl_2$ and 20× Sypro orange dye in a total volume of 10 µl in a white 384-well plate. Thermofluor analyses were performed and analyzed using the default 'Tm Calling' analysis found in the LightCycler 480 Software (release 1.5.0) (Roche).[21]

Enzyme assays in different pHs

TEAS and HPS were assayed at varying pH range (4.5–10) in BTP, sodium maleate, 2-(N-morpholino)ethanesulfonic acid (MES), BIS-TRIS methane (BT), piperazine-N,N′-bis(2-ethanesulfonic acid) (PIPES), 3-(*N*-morpholino) propanesulfonic acid (MOPS), MOPSO and sodium phosphate buffers. Enzyme assays were carried out in a total volume of 500 µl (0.1 µM enzyme, 5 mM $MgCl_2$, 10 mM pH buffer and 25 µM FPP) overlaid with 500 µl hexane. Next, 20 µl of 625 µM FPP was added to initiate enzyme reactions. Assays were allowed to continue overnight and products were recovered as detailed above. For TEAS, HPS, TEAS-M9 and HPS-M9 in BTP (pH range 8–9.5), a 500 µl reaction (0.2 µM enzyme, 5 mM $MgCl_2$, 10 mM BTP and 50 µM FPP) was overlaid with 70 µl hexane. FPP was added last and incubated overnight at room temperature.

Measurement of apparent k_{cat} values

A 500 µl reaction containing 10 mM BTP, pH 7.0, 5 mM $MgCl_2$, 25 µM FPP and 5 nM enzyme was overlaid with 500 µl hexane containing *p*-chlorotoluene (SUPELCO). After 8, 22 and 36 min of incubations at room temperature, the reaction mixtures were vortexed, phase separated and the top hexanes were injected into a Hewlett-Packard 6890 GC coupled to a 5973 mass selective detector equipped with an HP-5MS column in splitless mode. From preliminary experiments, the velocity of TEAS and HPS reactions using 25 µM FPP is ~80–90% of V_{max}, and thus 25 µM FPP was used for all proteins for apparent k_{cat} dzerivations with an assumption that their K_M values are similar.

Protein crystallization and data collection

TEAS crystals were grown in hanging drops with 1 µl of protein (20 mg ml^{-1}) and 1 µl of reservoir (100 mM MOPSO, pH 7.0, 200 mM magnesium acetate and 13% (w/v) PEG 8000) at 4 °C. TEAS crystals were transferred to a drop of reservoir solution containing FPP or (*E*,*E*)-farnesyl monophosphate (FMP) at final concentrations of 1.3 mM. The TEAS-M4 crystal grew under the same conditions as WT TEAS, and was transferred to a drop of reservoir solution containing 10 mM premnaspirodiene (**2**) in sealed wells and incubated over the same reservoirs including a layer of pure premnaspirodiene (**2**) oil. X-ray diffraction data were collected at beamlines BL8.2.1 and BL8.2.2 at Lawrence Berkeley National Laboratory (LBNL, Berkeley, CA, USA). Data were processed using imosflm,[22] the CCP4 Program Suite,[23] PHENIX[24] and COOT.[25]

RESULTS AND DISCUSSION

Analyses of TEAS, HPS, TEAS-M9 and HPS-M9 product profiles

The product profiles of TEAS, HPS, TEAS-M9 and HPS-M9 were analyzed using both nonpolar and chiral GC columns previously used to characterize TEAS products (Figure 2).[12] In order to simplify analyses of the minor products produced, terpenoids were grouped into product classes according to their presumed biosynthetic origin (Figure 1).[12] Products in class A originate from quenching of the (*E*,*E*)-farnesyl cation, class B from quenching the eudesmyl cation with no alkyl migrations, classes C1, C2 and C3 from a eudesmyl cation with alkyl migrations and class D from quenching the (*Z*,*E*)-farnesyl cation. Products that could not be identified by GC-MS-based fragmentation patterns and comparison with authentic standards were placed in class Z.

Overall, HPS biosynthesizes premnaspirodiene (**2**) at 95% of its total extractable terpenoid products (Table 1 and Supplementary Figure 2). Interestingly, and probably not surprisingly given their common evolutionary ancestry, almost all minor products identified in the profiles of HPS were also previously detected in the profiles of TEAS.[12] Comparing HPS products with the known TEAS product profiles, including GC column retention times and MS-based fragmentation patterns, confirmed the production of germacrene

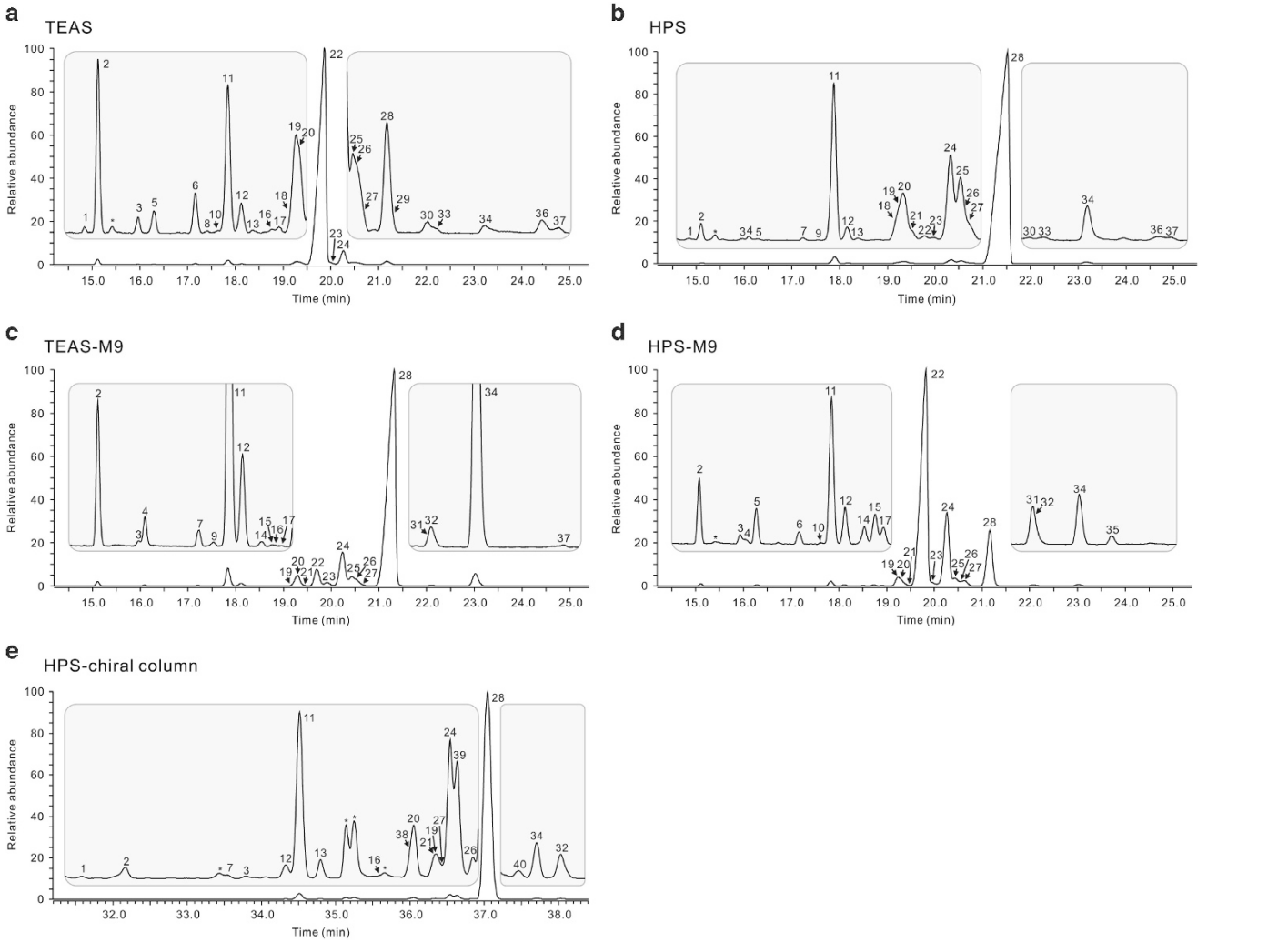

Figure 2 Total ion chromatograms of (**a**) *Nicotiana tabacum* 5-*epi*-aristolochene synthase (TEAS), (**b**) *Hyoscyamus muticus* premnaspirodiene synthase (HPS), (**c**) TEAS-M9 and (**d**) HPS-M9 products. Chromatogram (**e**) is the product profile of HPS when run on the chiral column. Inset panels enlarge minor products 30× at the corresponding retention time. Peak numbers correspond to products listed in Table 1.

A (**3**) (and subsequent thermal rearrangement to β-elemene (**4**)), 5-*epi*-aristolochene (**1**), 4-*epi*-eremophilene (**5**), spirolepechinene (**6**), α-selinene (**7**), premnaspirodiene (**2**) and α-cedrene (**8**).[12] β-Selinene (**9**) and α-selinene (**7**) were discerned using celery extract for standards, and β-curcumene (**10**) was identified by comparison with an authentic standard (Supplementary Figures 3 and 4). Products stemming from the (*Z*,*E*)-farnesyl diphosphate (alternatively (3*RS*)-nerolidyl diphosphate) are widely observed in other terpene synthases, such as amorpha-4,11-diene synthase[6] or α-zingiberene/β-sesquiphellandrene synthase.[26] Both mass spectra and retention times confirmed that HPS produces α-cedrene (**8**) but not α-acoradiene (**11**), although both are observed as products of TEAS.[27] An unknown compound (unknown-8) and an eremophila-1(10),6-diene-like product were produced by HPS and not TEAS. Analyses of the TEAS-M9 and HPS-M9 product profiles revealed a startling switch in product profiles for each mutant (Table 1). Although there were several new peaks that could not be identified, these constituted <1% of the total extractable products. Overall, the major products of these four enzymes arose from either a C14 methyl shift or a C8 methylene shift of the eudesmyl cation.

Although several compounds were identified using the mass spectral library and/or retention time indices, many products could not be confirmed. Unknown-7 bears strong resemblance to valencene or eremophilene (**12**) based on mass fragmentation data, and we classified it as a C1 product (Supplementary Figures 5 and 6). We classified some of the HPS products thought to be spirovetivadienes and eremophiladienes as unknown. From this study, we suggest the systematic naming of different spirovetivadienes and eremophiladienes by adding their chiralities in front of chemical names, and we also suggest naming of new possible unknown products, aristolochadienes (Supplementary Figure 7).

Temperature changes influence minor product profiles differently based on active site residues

The product profile of TEAS varied as a function of the reaction temperature.[12] Therefore, we compared the sensitivity of product profiles with temperature for TEAS, HPS, TEAS-M9 and HPS-M9 by measuring product profiles of enzymes incubated at temperatures ranging from 15 to 42.5 °C. To compare among all four TPSs, the change in product production for each class of compounds was

Table 1 Product profiles of TEAS, HPS, TEAS-M9 and HPS-M9

		Abundance (%)[a]					Retention time	
Peak	*HPS product*	*TEAS*	*HPS*	*TEAS-M9*	*HPS-M9*	*Validation*	*Normal*	*Chiral*
1	*cis*-β-elemene	0.034	0.017			Lib	14.9	31.48
2	β-elemene (**4**)	1.094	0.117	0.625	0.307	O'Maille *et al.*[12]	15.14	32.16
3	α-cedrene (cedr-8-ene) (**8**)	0.107	0.012	0.021	0.047	Faraldos *et al.*[27]	15.99	33.77
4	spirovetiva-1(10),6-diene		0.029	0.140	0.025	Lib	16.14	
5	(*E*)-caryophyllene	0.176	0.015		0.181	Lib	16.32	
6	Unknown-1	0.309			0.070		17.17	33.77
7	Unknown-2 (eremophila-1(10),6-diene-like)		0.019	0.083			17.24	33.54
8	selina-5,11-diene	0.018				Lib	17.42	
9	Unknown-8		0.003	0.025			17.57	
10	Unknown-9	0.019			0.005		17.65	
11	spirolepechinene (**6**)	1.298	1.436	3.223	0.861	Lib	17.89	34.51
12	Unknown-3	0.265	0.121	0.536	0.213		18.17	34.32
13	(*E*)-β-farnesene	0.029	0.019			Lib	18.38	34.8
14	Unknown-10 (eremophila-1(10),7-diene-like)			0.027	0.112		18.52	
15	Unknown-11			0.008	0.205		18.73	
16	α-acoradiene (**11**)	0.038		0.004		Faraldos *et al.*[27]	18.78	35.61
17	4,5-di-*epi*-aristolochene	0.053		0.005	0.107	Lib	18.92	35.8
18	Unknown-4	0.025	0.233				19.19	
19	Unknown-5	0.482	0.155	0.130	1.476		19.28	36.35
20	selina-4,11-diene	1.031	0.423	2.452	1.184	Lib	19.35	36.04
21	Unknown-6		0.076	0.056	0.043		19.51	36.29
22	5-*epi*-aristolochene (**1**)	87.158	0.050	3.763	60.134	O'Maille *et al.*[12]	19.77	36.45
23	β-selinene (**9**)	0.408	0.026	0.851	0.656	Celery extract	19.97	37.02
24	4-*epi*-eremophilene (**5**)	4.309	1.039	8.408	16.983	O'Maille *et al.*[12]	20.3	36.53
25	Unknown-7 (valencene-like)	0.584	0.762	2.291	1.718		20.51	
26	α-selinene (**7**)	0.663	0.097	1.027	0.259	Celery extract	20.65	36.84
27	(−)-hinesene	0.066	0.073	0.053	1.271	Lib	20.74	36.44
28	premnaspirodiene (**2**)	1.213	94.697	72.931	13.329	O'Maille *et al.*[12]	21.17	37.05
29	(−)-helminthogermacrene	0.065				Lib	21.3	38.03
30	β-curcumene (**10**)	0.114	0.026			std	21.91	
31	Unknown-12			0.097	0.327		22.1	
32	Unknown-13 (7-*epi*-α-selinene-like)			0.057	0.029		22.14	38.16
33	Unknown-14	0.055	0.034				22.19	
34	Unknown-15 (spirovetiva-1(10),7(11)-diene-like)	0.121	0.470	3.169	0.397		23.11	37.7
35	Unknown-16				0.063		23.68	
36	Unknown-17	0.189	0.007				24.62	
37	Unknown-18	0.076	0.044	0.019			24.86	
38	Unknown-19							36.01
39	Unknown-20 (eremophilene-like)							36.63
40	Unknown-21							37.46

Abbreviations: HPS, *Hyoscyamus muticus* premnaspirodiene synthase; Lib, from the library search; std, from the comparison with authentic standard; TEAS, *Nicotiana tabacum* 5-*epi*-aristolochene synthase.
Major products are highlighted in grey, with a darker grey color indicating greater production.
[a]Product abundance is based on products in nonpolar column.

graphed against temperature (Figure 3). These data were further analyzed to easily compare changes in product profile for each TPS (Supplementary Figure 8). Overall, the HPS product profile was much less temperature sensitive than that of TEAS. TEAS-M9 and HPS-M9 possess temperature sensitivities that lie between wild-type TEAS and HPS. Notably, HPS retained the C8 methylene migration to form its major product premnaspirodiene (**2**) at elevated temperatures, only exhibiting an increase in products arising from the TEAS-like methyl shift rearrangement. This suggests that the HPS active site and its immediate environment possess altered flexibility relative to TEAS. TEAS, HPS-M9 and TEAS-M9 showed an increase in class A and class B products, arising from failure to form the eudesmyl cation and proton loss from the eudesmyl cation, respectively. These observations suggest that these latter TPSs retaining an overall TEAS sequence maintain more flexible active sites that are unable to facilitate proper cation formation and rearrangements as temperatures increase. Interestingly, *Callitropsis nootkatensis* CnVS and *Citrus sinensis* CitrusVS, both valencene synthases, produced more germacrene A (**3**) at higher temperature, similar to our observation of increased class A compounds at high temperatures.[17]

Overall protein thermostability is minimally affected by active site mutations

After heat treatments at a given temperature for up to 16 min, reactions were carried out for all 4 TPSs and total product

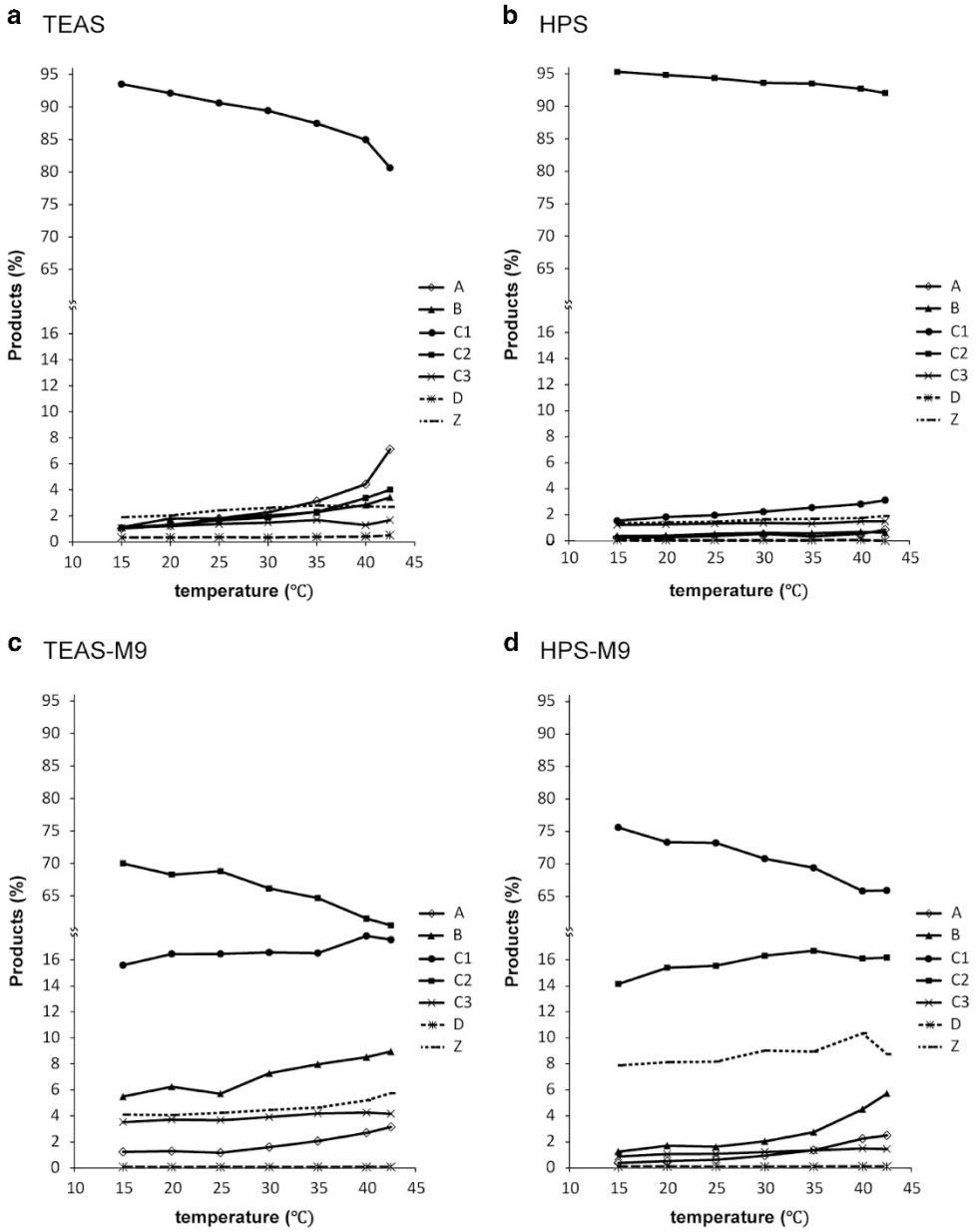

Figure 3 Product classification of (**a**) *Nicotiana tabacum* 5-*epi*-aristolochene synthase (TEAS), (**b**) *Hyoscyamus muticus* premnaspirodiene synthase (HPS), (**c**) TEAS-M9 and (**d**) HPS-M9 at different temperatures. Products were quantified and classified according to the structures found in Figure 1.

formations were measured. The overall product output for TEAS and TEAS-M9 begins to decrease at 45 °C, but HPS and HPS-M9 lose activity at 40° (Supplementary Figure 9). The data are linear when graphed on the log scale. The slopes from natural log values clearly show that TEAS and TEAS-M9 are more resistant to heat inactivation than HPS and HPS-M9. Interestingly, a previously studied TEAS variant with 12 mutations, called Thermo-TEAS, is active at 65 °C and has a greater thermostability than wild-type TEAS.[28] However, mutations in thermo-TEAS are not located around the active site, and thermo-TEAS produces a larger amount of minor products than wild type. Therefore, differences between the surface residues of TEAS and HPS may account for thermostability, and thermostability does not directly correlate with product profile diversity.

High pH increases minor product production

TEAS and HPS exhibit altered product profiles at different pH values (Supplementary Figure 10). TEAS activity was assessed between pH 4.5 and 9.5, and HPS between pH 5 and 10 (Supplementary Figure 11). Overall, the TEAS product profile changes more as pH varies than that of HPS, but both profiles began to significantly change when pH values above 8 are tested. Between pH 8 and 9.5, TEAS produced a greater proportion of minor products relative to 5-*epi*-aristolochene (**1**), whereas HPS produced over 80% premnaspirodiene (**2**). Product profiles of TEAS, HPS, TEAS-M9 and HPS-M9 were analyzed in the pH range of 8 to 9.5 (Figure 4). Similar to the effect of temperature on product class profiles, HPS exhibited the least change in the product profile, and TEAS, HPS-M9 and TEAS-M9 showed similar and larger degrees of change.

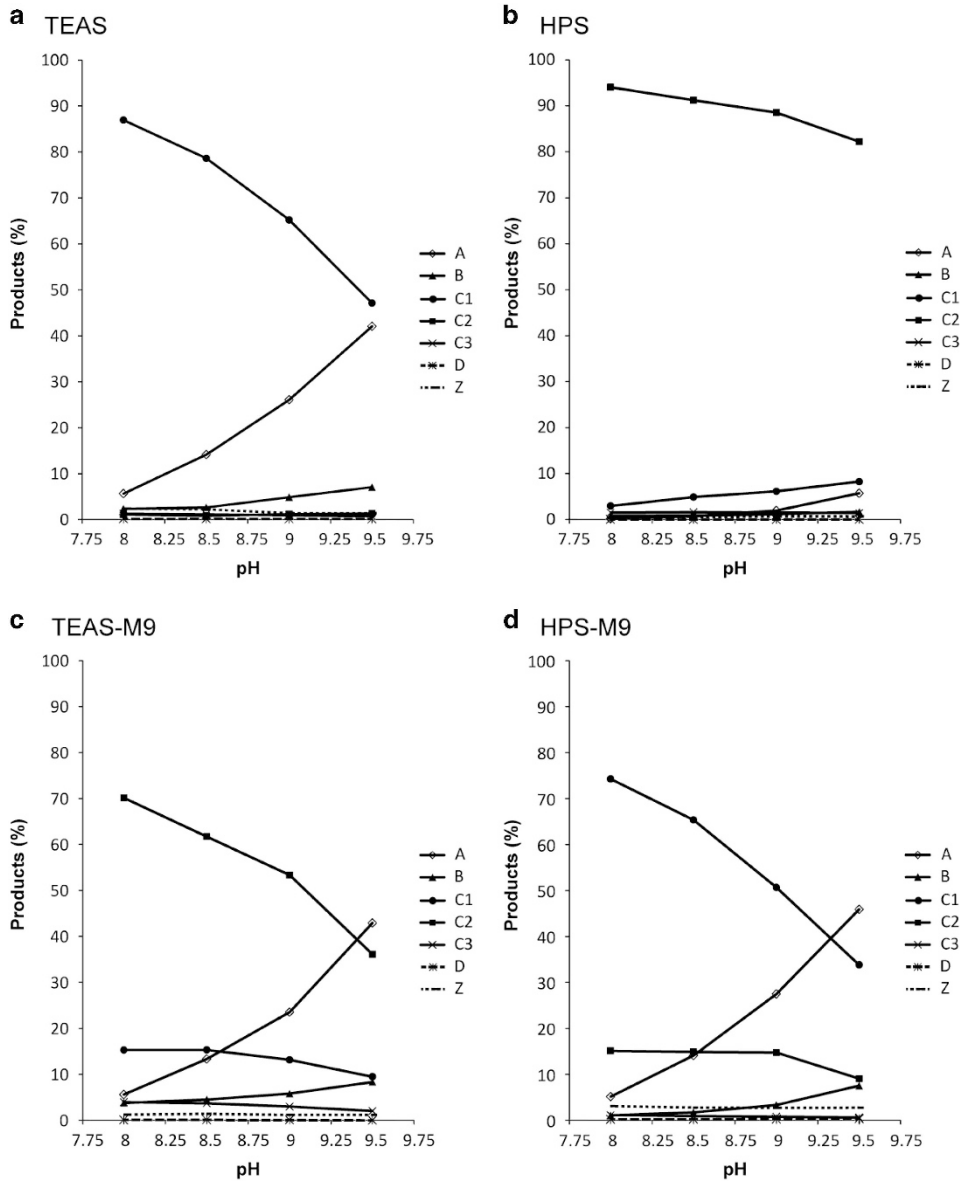

Figure 4 Product classification of (**a**) *Nicotiana tabacum* 5-*epi*-aristolochene synthase (TEAS), (**b**) *Hyoscyamus muticus* premnaspirodiene synthase (HPS), (**c**) TEAS-M9, and (**d**) HPS-M9 at different pH in Bis-Tris propane buffer. Products were quantified and classified according to the structures found in Figure 1.

More specifically, a large increase in class A products, which arise from failure to reach the eudesmyl cation intermediate, were observed for these three enzymes (supplementary Figure 12). High pH may modulate the required protonation of the C6-C7 double bond of germacrene A (**3**) for eudesmyl cation formation. In addition, Y520 of TEAS has been implicated in the reprotonation of germacrene A (**3**), and the proton donating capacity of the phenolic hydroxyl moiety of this tyrosine is most likely affected by high pH and its intrinsic pK_a.[29]

Similarly, the fungal TPS Cop4, which normally produces δ-cadinene, generates much higher levels of germacrene D when the H-α1 loop containing a putative proton donor His that spans the active site is altered.[18] Therefore, altering the histidine residue greatly increases germacrene D formation. This example bears remarkable similarity to Y520 in TEAS in which pH would affect the protonation state of these residues. Moreover, increased pH or mutations in this area of the enzyme may also destabilize the J-K loop, a flexible loop that spans the active site cavity in TEAS (Figure 5), inducing release of early termination products from TPSs.

Relationship between enzyme activity and TPS thermostability

Thermal stabilities of each TPS were measured over a range of pH values by using the dye-based Thermofluor assay, whereby melting temperatures (T_m) are calculated (Supplementary Figure 13).[21] TEAS, HPS, TEAS-M9 and HPS-M9 exhibited an average T_m of 35.8, 38.7, 45.2 and 46.3 °C, respectively. TPSs with low thermal stability in the Thermofluor assay possess greater apparent k_{cat} values. Average apparent k_{cat} values of TEAS, HPS, TEAS-M9 and HPS-M9 are 16.4 min^{-1}, 20.8 min^{-1}, 11.8 min^{-1} and 2.8 min^{-1}, respectively. Higher TPS stability may be associated with the rigidity of the J-K loop that then results in lower enzyme activity because of slow product release. Mutations of the M9 positions in both TEAS and HPS result in lower enzyme activities, but higher T_ms. Examination of the pH

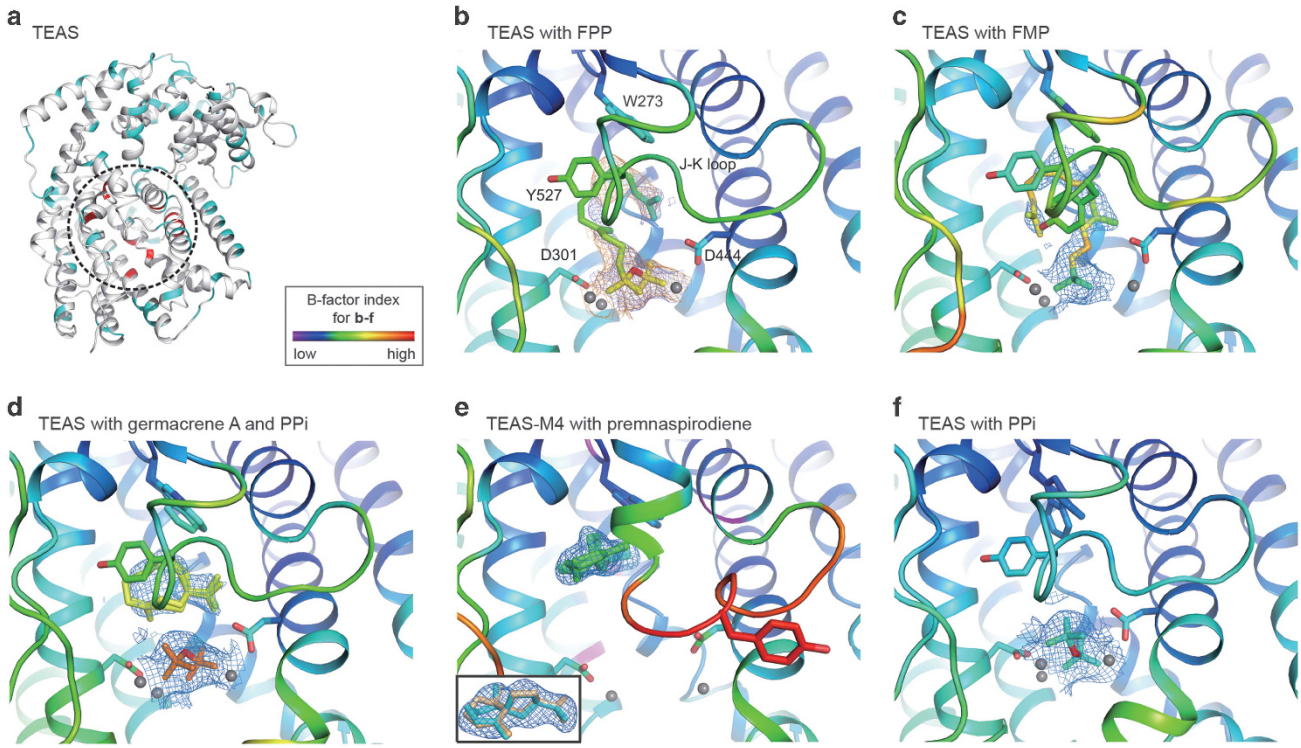

Figure 5 Structural details of *Nicotiana tabacum* 5-*epi*-aristolochene synthase (TEAS) and TEAS quadruple mutant crystal structures solved and refined as part of this study. (**a**) Overall structure of TEAS, with residues in blue and red representing differences between TEAS and *Hyoscyamus muticus* premnaspirodiene synthase (HPS). The red residues are the 9 positions that differ in each M9 mutant. The active site is indicated by a dotted circle. Inset denotes the atomic displacement parameters (ADPs or B-factors) color scale for the remaining panels. (**b**) Structure of TEAS with farnesyl diphosphate (FPP) bound. (**c**) Structure of TEAS with (*E*,*E*)-farnesyl monophosphate (FMP) bound. (**d**) Structure of TEAS with germacrene A and pyrophosphate (PPi) bound. (**e**) Structure of a TEAS quadruple mutant with premnaspirodiene bound. Inset details the electron density associated with the premnaspirodiene. (**f**) Structure of TEAS with PPi bound.

effects on both T_ms and apparent k_{cat}s reveals a clear difference between TEAS and HPS backgrounds. The optimal pH for TEAS shifts from pH 6.25 to pH 7.5 upon mutation to TEAS-M9, whereas it remains almost the same (pH 6.75 and pH 6.5) for HPS and HPS-M9 (Supplementary Figure 13). Similarly, the optimal pH for stability of TEAS shifts from pH 8.5 to pH 7 in TEAS-M9, whereas HPS and HPS-M9 have the same optimal pH. Here, the pH values for highest enzyme activities and thermal stabilities of TEAS and TEAS-M9 also show inverse relationships for apparent k_{cat}s and K_ms. Taken together, these data suggest that increased TPS stability correlates with decreased turnover number and decreased diversity in minor products formed.

Structural analysis of TEAS bound with small molecules

In order to investigate structural properties that affect carbocation formation and product cyclization, TEAS and a mutant containing four mutations were crystallized and crystals soaked with a variety of substrates and products (Figure 5a). As TEAS is functional in crystallization buffer in the presence of Mg^{2+}, FPP soaked into TEAS crystals is often ionized, and typically only PP remains visible in the active site. Therefore, we varied soaking times of FPP into TEAS crystals at 4 °C in order to trap the intact FPP molecule in the active site and succeeded in this effort (Figure 5b). This is the first report of FPP coordinated with Mg^{2+} ions in a TPS-active site. To solve these structures, simulated annealing was used to fit FPP into electron density in the active site. Similarly, FMP was soaked into the active site of TEAS (Figure 5c). The density of the C1 and C2 carbons aided in modeling the direction in which the farnesyl chain folds. Interestingly, the farnesyl chains of FPP and FMP fold in opposite directions. The directionality of FMP matches that of farnesyl hydroxyphosphate (Protein Data Bank (PDB) ID, 5EAT) and the directionality of FPP matches that of trifluoro-farnesyl diphosphate (PDB ID, 5EAU).[30]

The electron density of FPP near the pyrophosphate is well ordered, but electron density for the remaining carbon chain remains partially disordered. This suggests that FPP is held very tightly at the pyrophosphate end by the three Mg^{2+} ions visible in the active site, whereas the carbon chain is free to adopt different conformations in the relatively spacious active site. Upon C-O bond cleavage, the carbon chain, now free from its pyrophosphate tether, 'snaps' into a conformation that facilitates double bond capture of the allylic farnesyl cation and formation of the cyclic germacryl cation. The terminal carbons that form the isopropenyl moiety of germacrene A (**3**) are in an almost identical conformation as observed in the FPP-soaked structure (Figure 5d). A recent computational analysis of the TEAS active site confirms the importance of this 'pre-Germacrene' conformation of FPP.[31] The 'U-shape' of FPP observed in the active site of our crystal structure is induced by the coordination of the pyrophosphate by the three Mg^{2+} ions. The U shape is important for the conformation of the J-K loop, and more specifically, proper orientation of Y527. In addition, the conformation of germacrene A (**3**) in TEAS correlates well with the proposed conformations of substrate intermediates in which Y527 is positioned over germacrene A (**3**) and pyrophosphate bound in the active site.[32]

A TEAS quadruple active site mutant[15] (A274T, V372I, Y406L, V516I) soaked with premnaspirodiene (**2**) exhibits a highly disordered J-K loop, indicating that as this product forms, the J-K loop moves to accommodate product formation and subsequent release (Figure 5e).

This is supported by the observation that the unequivocal electron density associated with premnaspirodiene (**2**) now occupies the space that Y527 did in both the FPP and germacrene A (**3**) bound structures. TEAS shields the carbocation and downstream carbocation transformations from bulk solvent with the J-K until the final product forms, at which time the product is released by 'pushing' the J-K loop out of position to release the final product. Increasing temperature or pH may destabilize the J-K loop, and therefore products have a higher likelihood of being released before their final cyclization and/or neutralization by proton loss. This would account for the increase in minor products at high temperatures and pH conditions, especially the observation of increased germacrene A (**3**) production. However, the broadening of TPS product profiles could be independent of the J-K loop and may be simply due to altered dynamics and shape of the active site. Although the crystal structures may not completely explain product profile alterations under extreme conditions, it is important to note the difference in the J-K loop position when comparing FPP, germacrene A (**3**) and premnaspirodiene (**2**) bound TEAS structures. This provides insight into product formation and release independent of pH or temperature conditions.

CONCLUSION

TPSs are responsible for producing a wide variety of terpenoid-based natural products. However, they often exhibit diverse product profiles. We characterized the product profiles of Egyptian henbane HPS and two previously described mutant TPSs TEAS-M9 and HPS-M9.[16] We also investigated TPS product profiles as a function of changing environmental perturbations, including temperature and pH. Further structural investigation of substrate-bound TEAS provides structural evidence of the importance of the J-K loop conformations and dynamics in TPSs, providing a partial structural rationale for diverse product profiles. This information will allow us to better understand the control of carbocation rearrangements by TPSs as a function of natural sequence variation in diverging lineages of related TPSs.

HPS exhibited tighter control over minor product formation than TEAS. The product profile of TEAS is altered more than that of HPS when varying temperature and pH, suggesting that TEAS possesses a more dynamic enzyme fold that results in greater structural variation of the active site as extrinsic environmental conditions change. This is particularly important for sessile plants that operate in widely varying ecological niches. Therefore, TEAS may be more favorably positioned as an 'evolvable' TPS, as it is capable of producing nontrivial quantities of minor products, whereas HPS is a more 'specialized' TPS with a narrower product profile.

As temperature increases, TEAS produces early-termination minor products at higher proportions than HPS, specifically products that result from premature proton loss and neutralization. We propose that increasing temperature subsequently enhances the movement of the flexible J-K loop, leading to escape of early termination products or their penultimate carbocations from the active site. The protonation state of Y520, a residue with a putative role in proton shuttling to the germacrene A (**3**) intermediate in TEAS, may be acutely affected at different pH values. Furthermore, pH could also modulate the positioning of Y527, a tyrosine located on a highly mobile stretch of the J-K loop that may in turn affect the stabilization of carbocations and the dynamics of the J-K loop as a whole. Our structural analyses of product precursor molecules complexed with TEAS provide structural bases for product formation and final cyclization, as well as potential structural effects of temperature and pH changes on TPS structure and function. Our insight into TPS product biosynthesis not only increases a basic understanding of the complex effect of enzyme dynamics and primary structure on product profiles, but also brings to light properties that are subject to directed evolution and natural evolution in the selection and control of TPS product formation. This is most notable in TPSs displaying a very recent divergence from a common ancestor such as is the case for TEAS and HPS from two closely related Solanaceous species.

CONFLICT OF INTEREST

The authors declare no conflict of interest.

ACKNOWLEDGEMENTS

Research in our laboratories is supported by NSF EEC-0813570 to JPN and NSF IOS1516156 to MDB. JPN is an investigator with the Howard Hughes Medical Institute.

1 Lange, B. M. The evolution of plant secretory structures and emergence of terpenoid chemical diversity. *Annu. Rev. Plant Biol.* **66**, 139–159 (2015).
2 Cane, D. E. & Ikeda, H. Exploration and mining of the bacterial terpenome. *Acc. Chem. Res.* **45**, 463–472 (2012).
3 Degenhardt, J., Köllner, T. G. & Gershenzon, J. Monoterpene and sesquiterpene synthases and the origin of terpene skeletal diversity in plants. *Phytochemistry* **70**, 1621–1637 (2009).
4 Vickery, C. R., La Clair, J. J., Burkart, M. D. & Noel, J. P. Harvesting the biosynthetic machineries that cultivate a variety of indispensable plant natural products. *Curr. Opin. Chem. Biol.* **31**, 66–73 (2016).
5 García, A., Bocanegra-García, V., Palma-Nicolás, J. P. & Rivera, G. Recent advances in antitubercular natural products. *Eur. J. Med. Chem.* **49**, 1–23 (2012).
6 Bouwmeester, H. J. *et al.* Amorpha-4,11-diene synthase catalyses the first probable step in artemisinin biosynthesis. *Phytochemistry* **52**, 843–854 (1999).
7 Raut, J. S., Shinde, R. B., Chauhan, N. M. & Mohan Karuppayil, S. Terpenoids of plant origin inhibit morphogenesis, adhesion, and biofilm formation by Candida albicans. *Biofouling* **29**, 87–96 (2013).
8 Wani, M. C., Taylor, H. L., Wall, M. E., Coggon, P. & McPhail, A. T. Plant antitumor agents. VI. Isolation and structure of taxol, a novel antileukemic and antitumor agent from Taxus brevifolia. *J. Am. Chem. Soc.* **93**, 2325–2327 (1971).
9 Major, D. T., Freud, Y. & Weitman, M. Catalytic control in terpenoid cyclases: multiscale modeling of thermodynamic, kinetic, and dynamic effects. *Curr. Opin. Chem. Biol.* **21**, 25–33 (2014).
10 Miller, D. J. & Allemann, R. K. Sesquiterpene synthases: passive catalysts or active players? *Nat. Prod. Rep.* **29**, 60–71 (2012).
11 Christianson, D. W. Unearthing the roots of the terpenome. *Curr. Opin. Chem. Biol.* **12**, 141–150 (2008).
12 O'Maille, P. E., Chappell, J. & Noel, J. P. Biosynthetic potential of sesquiterpene synthases: alternative products of tobacco 5-epi-aristolochene synthase. *Arch. Biochem. Biophys.* **448**, 73–82 (2006).
13 Cane, D. E., Prabhakaran, P. C., Oliver, J. S. & McIlwaine, D. B. Aristolochene biosynthesis. Stereochemistry of the deprotonation steps in the enzymatic cyclization of farnesyl pyrophosphate. *J. Am. Chem. Soc.* **112**, 3209–3210 (1990).
14 Back, K. & Chappell, J. Cloning and bacterial expression of a sesquiterpene cyclase from hyoscyamus muticus and its molecular comparison to related terpene cyclases. *J. Biol. Chem.* **270**, 7375–7381 (1995).
15 Greenhagen, B. T., O'Maille, P. E., Noel, J. P. & Chappell, J. Identifying and manipulating structural determinates linking catalytic specificities in terpene synthases. *Proc. Natl Acad. Sci. USA* **103**, 9826–9831 (2006).
16 O'Maille, P. E. *et al.* Quantitative exploration of the catalytic landscape separating divergent plant sesquiterpene synthases. *Nat. Chem. Biol.* **4**, 617–623 (2008).
17 Beekwilder, J. *et al.* Valencene synthase from the heartwood of Nootka cypress (*Callitropsis nootkatensis*) for biotechnological production of valencene. *Plant Biotechnol. J.* **12**, 174–182 (2014).
18 López-Gallego, F., Wawrzyn, G. & Schmidt-Dannert, C. Selectivity of fungal sesquiterpene synthases: role of the active site's H-1α loop in catalysis. *Appl. Environ. Microbiol.* **76**, 7723–7733 (2010).
19 Köllner, T. G. *et al.* Protonation of a neutral (S)-β-bisabolene intermediate is involved in (S)-β-macrocarpene formation by the maize sesquiterpene synthases TPS6 and TPS11. *J. Biol. Chem.* **283**, 20779–20788 (2008).
20 Kulkarni, R. S., Chidley, H. G., Pujari, K. H., Giri, A. P. & Gupta, V. S. Geographic variation in the flavour volatiles of Alphonso mango. *Food Chem.* **130**, 58–66 (2012).
21 Ericsson, U. B., Hallberg, B. M., DeTitta, G. T., Dekker, N. & Nordlund, P. Thermofluor based high-throughput stability optimization of proteins for structural studies. *Anal. Biochem.* **357**, 289–298 (2006).
22 Leslie, A. G. W. Recent changes to the MOSFLM package for processing film and image plate data. *Joint CCPS ESF-EAMCB Newsl. Prot. Crystallogr.* **26**, 27–33 (1992).
23 Winn, M. D. *et al.* Overview of the *CCP* 4 suite and current developments. *Acta Crystallogr.* **67**, 235–242 (2011).

24 Adams, P. D. *et al. PHENIX*: a comprehensive Python-based system for macromolecular structure solution. *Acta Crystallogr.* **66**, 213–221 (2010).
25 Emsley, P. & Cowtan, K. *Coot*: model-building tools for molecular graphics. *Acta Crystallogr.* **60**, 2126–2132 (2004).
26 Koo, H. J. & Gang, D. R. Suites of terpene synthases explain differential terpenoid production in ginger and turmeric tissues. *PLoS ONE* **7**, e51481 (2012).
27 Faraldos, J. A., O'Maille, P. E., Dellas, N., Noel, J. P. & Coates, R. M. Bisabolyl-derived sesquiterpenes from tobacco 5-epi-aristolochene synthase-catalyzed cyclization of (2Z,6E)-farnesyl diphosphate. *J. Am. Chem. Soc.* **132**, 4281–4289 (2010).
28 Diaz, J. E. *et al.* Computational design and selections for an engineered, thermostable terpene synthase. *Protein Sci.* **20**, 1597–1606 (2011).
29 Rising, K. A., Starks, C. M., Noel, J. P. & Chappell, J. Demonstration of germacrene A as an intermediate in 5-epi-aristolochene synthase catalysis. *J. Am. Chem. Soc.* **122**, 1861–1866 (2000).
30 Starks, C. M., Back, K., Chappell, J. & Noel, J. P. Structural basis for cyclic terpene biosynthesis by tobacco 5-epi-aristolochene synthase. *Science* **277**, 1815–1820 (1997).
31 Zhang, F., Chen, N. & Wu, R. Molecular dynamics simulations elucidate conformational dynamics responsible for the cyclization reaction in TEAS. *J. Chem. Inf. Model.* **56**, 877–885 (2016).
32 O'Brien, T. E., Bertolani, S. J., Tantillo, D. J. & Siegel, J. B. Mechanistically informed predictions of binding modes for carbocation intermediates of a sesquiterpene synthase reaction. *Chem. Sci.* (2016).

Supplementary Information accompanies the paper on The Journal of Antibiotics website (http://www.nature.com/ja)